RapA, the SWI/SNF Subunit of *Escherichia coli* RNA Polymerase, Promotes the Release of Nascent RNA from Transcription Complexes[†]

Brandon Yawn,[‡] Lin Zhang,[‡] Cameron Mura,[§] and Maxim V. Sukhodolets*[,‡]

[‡]*Department of Chemistry, Lamar University, Beaumont, Texas 77710, and* [§]*Department of Chemistry, University of Virginia, Charlottesville, Virginia 22904*

ABSTRACT: RapA, a prokaryotic member of the SWI/SNF protein superfamily, is an integral part of the RNA polymerase transcription complex. RapA's function and catalytic mechanism have been linked to nucleic acid remodeling. In this work, we show that mutations in the interface between RapA's SWI/SNF and double-stranded nucleic acid-binding domains significantly alter ATP hydrolysis in purified RapA. The effects of individual mutations on ATP hydrolysis loosely correlated with RapA's nucleic acid remodeling activity, indicating that the interaction between these domains may be important for the RapA-mediated remodeling of nonproductive transcription complexes. In this study, we introduced a model system for in vitro transcription of a full-length *Escherichia coli* gene (*slyD*). To study the function of RapA, we fractionated and identified in vitro transcription reaction intermediates in the presence or absence of RapA. These experiments demonstrated that RapA contributes to the formation of free RNA species during in vitro transcription. This work further refines our models for RapA function in vivo and establishes a new role in RNA management for a representative of the SWI/SNF protein superfamily.

Escherichia coli has served as a primary model system for the study of enzymes involved in RNA synthesis. A textbook example of polymerase function, the *E. coli* core RNA polymerase formed by the $\alpha_2\beta\beta'\omega$ subunits is capable of transcription elongation and termination (*1*). Proteins called sigma factors (*1*−*3*) associate with the core enzyme and allow the resulting complex, termed the RNA polymerase holoenzyme, to bind DNA in a sequence-specific manner and initiate transcription from loosely homologous promoter sequences on the *E. coli* chromosome. Each sigma factor controls multiple groups of promoters; e.g., the key growth-related and housekeeping genes in *E. coli* are under control of σ^{70} (*4*), the *rpoD* gene product. Approximately one-third of the core *E. coli* RNA polymerase molecules in a given cell form a high-affinity, stoichiometric complex with σ^{70} under normal growth conditions; the $\alpha_2\beta\beta'\omega$ and $\alpha_2\beta\beta'\omega\sigma^{70}$ enzyme species display a number of distinct properties and can be chromatographically separated (*5*, *6*). Apart from the sigma factors and relatively small proteins (which are unlikely to display mechanistically complex enzymatic activities), the key known interactors of the *E. coli* RNA polymerase established through biochemical studies are NusA (*7*, *8*) and RapA (*6*, *9*). NusA, an essential RNA-binding protein in *E. coli*, has been described in the existing literature as a transcription elongation factor and a cofactor of antiterminators (*10*−*13*). The function of RapA (also known as HepA), the

first identified bacterial representative of the SWI/SNF protein superfamily, is not fully understood. Under most conditions (in liquid cultures), *rapA* deletion has little or no effect on cell growth (*6*, *14*), protein expression [as judged by two-dimensional electrophoresis (M. V. Sukhodolets, unpublished results)], UV sensitivity (*14*), or mutation rates (*14*). This apparent lack of a pronounced *rapA* effect in vivo points to functions other than general regulation of transcription, as proposed for RapA's eukaryotic counterparts. However, *rapA* deletion results in a unique phenotype, rendering bacteria incapable of efficient growth on agar plates in high salt (*15*). In vitro, RapA promotes multiround transcription in a salt concentration-specific fashion (*15*, *16*). Salt selectivity is therefore a shared feature of RapA effects observed in vivo and in vitro. Our recent work presented multiple, independent lines of evidence indicating that RapA binds and remodels RNA during transcription (*17*). This study also indicated that noncanonical DNA−RNA complexes such as DNA−RNA triplexes, the formation of which is enhanced in high salt (*17*), could represent potential substrates for RapA, and we proposed that remodeling of noncanonical nucleic acid complexes could be the primary function of RapA and its homologues in vivo (*17*). A recently reported, 3.2 Å resolution structure of RapA was used to construct a putative structural model for a RapA−nucleic acid complex, suggesting that RapA is capable of simultaneous interactions with both double-stranded and single-stranded nucleic acids (*18*). This is consistent with the proposed role of RapA in the remodeling of noncanonical nucleic acid complexes.

In this work, we construct several new RapA mutations, focusing on the RapA domain harboring SWI/SNF homology motifs IV−VI (herein termed the SWI/SNF domain) and its interface with the domain containing the putative double-stranded nucleic acid template (dsT) binding site (*17*, *18*), and studied their effect on RapA's ATP hydrolytic and nucleic acid

*To whom correspondence should be addressed. E-mail: msoukhodol@my.lamar.edu. Phone: (409) 880-7905 (office) or (409) 880-7906 (laboratory).

remodeling activities. We demonstrate a significant effect of the mutations in this region on RapA's ATP hydrolytic and nucleic acid remodeling activities. The effects of individual mutations on ATP hydrolysis loosely correlated with RapA's nucleic acid remodeling activity in in vitro transcription, indicating that the interaction between the SWI/SNF and dsT binding domains may be important for the RapA-mediated remodeling of nonproductive transcription complexes.

In this study, we have tested, for the first time in studies with RapA, the effects of RapA on the transcription of a model full-length *E. coli* mRNA containing intact 5′- and 3′-nontranslated sequences. The results presented herein are in accord with our existing model, in which RapA aids RNA polymerase in the displacement of nascent RNA from transcription complexes. We show that this enzymatic activity of RapA is unique and cannot be mimicked by other RNA binding proteins with a demonstrated ability to promote transcriptional cycling, such as S1 (*19*). In this work, we further develop our methods for fractionation and identification of in vitro transcription reaction intermediates. Using a nondenaturing (as well as a previously developed semidenaturing) method of separation of the in vitro transcription reaction intermediates, we demonstrate that RapA promotes the formation of non-DNA-bound or non-aggregated RNA species during transcription. This work further refines our models for RapA function in vivo and, taken together with our previous study, establishes a new role in RNA management for a representative of the SWI/SNF protein superfamily. This finding not only improves our understanding of the fundamental process of transcription but also brings a fresh perspective to studies demonstrating links between mutations in human SWI/SNF genes and cancer (*20*−*24*).

MATERIALS AND METHODS

Enzymes. In this study, we have further improved the procedure for the isolation of native *E. coli* RNA polymerase and its accessory proteins. The modified procedure, in general reminiscent to that described in ref *25*, results in improved purity of the isolated proteins and complexes. The key changes, in comparison with the protocol described in ref *25*, included (a) the utilization of two different FPLC[1] instruments [a classic (now discontinued) FPLC system (Pegasus Scientific), set up in the cold room to carry out the initial, single-stranded DNA chromatography stage, and an ACTA FPLC system (GE Healthcare) set up and operated at room temperature via Unicorn software during the final chromatography stages (however, the Superloops were placed on ice during the Mono Q column loading stage)], (b) the utilization of self-prepared (calf thymus) single-stranded DNA-Sepharose 4B instead of commercially available DNA-agarose, to improve flow rates, (c) scaling down the procedure to 25−35 g of *E. coli* MG1655 cells per purification and using a Mono Q 5/5 column to achieve more uniform loading of the column, and (d) increasing the length (>2-fold) of the Superdex 200 column during the final, gel exclusion chromatography stage. The schematic for the procedure is shown in Figure S1B of the Supporting Information;

---

[1]Abbreviations: CTP, cytidine 5′-triphosphate; ds, double-stranded; FPLC, fast protein liquid chromatography; GTP, guanosine 5′-triphosphate; PAGE, polyacrylamide gel electrophoresis; PCR, polymerase chain reaction; PEI, polyethylenimine; PBS, phosphate-buffered saline; PBST, PBS-Tween; RNAP, RNA polymerase; ss, single-stranded; TBE, Tris-borate-EDTA; TLC, thin layer chromatography; UTP, uridine 5′-triphosphate.
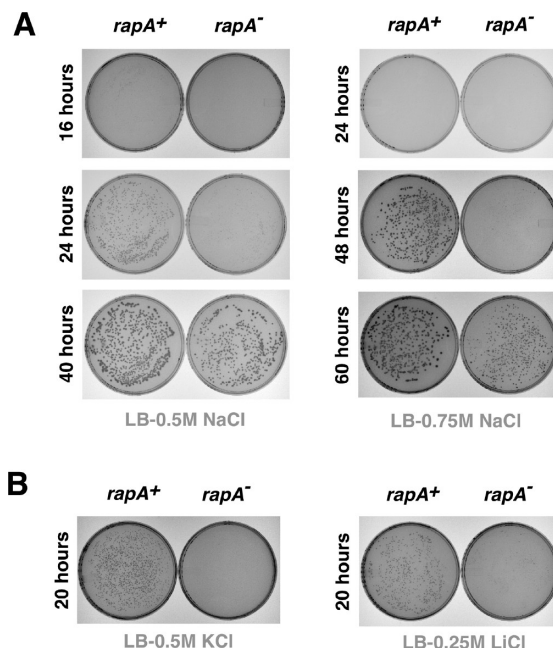

FIGURE 1: In vivo effects of the *rapA* deletion mutation. (A) Kinetics of the growth of *E. coli* MG1655*rapA*$^+$ and MG1655*rapA*$^-$ cells on LB agar plates containing elevated concentrations of sodium chloride. (B) Effects of KCl and LiCl on the growth of the two strains on LB agar.

the detailed protocol will be described elsewhere. Recombinant, His-tagged wild-type and mutant RapA proteins were purified as described in Figures S1C and S2 of the Supporting Information. Wild-type recombinant S1 and NusA were isolated as previously described (*25*).

PCR and DNA Purification. DNA encompassing the *slyD* operon was amplified from MG1655 *E. coli* chromosomal DNA using MS696 (5′-ATTGTAAGCTTCCCGGGGAAACGC-CACCGCCACATTATTGAGGCG) and MS697 (5′-CCGA-AAGTGGATCCCGGGGCCCGGCCTGTCAGGCGCAG-GATTCAATGGCG) DNA primers and the Expand High Fidelity PCR kit (Roche Diagnostics). Reactions were conducted as suggested by the manufacturer; the extension time was 2 min at 72 °C. Because our previous work implied the possibility of noncanonical interactions between nucleic acids in transcription, we tested different methods for purification of PCR-generated DNA templates to rule out potential impurity and/or conformational heterogeneity in the isolated DNA; the amplified DNA used in key experiments was purified by FPLC, as described in Figure S1 of the Supporting Information, using a custom-packed 0.3 mL Source Q column. Following DNA amplification, the reaction mixture was diluted 4−5-fold with purified water (KD Medical, molecular biology grade) and injected onto the column. The reaction products were eluted with a linear gradient of NaCl (from 0 to 1 M) in 20 mL of TGED buffer [0.01 M Tris-HCl, 5% glycerol, 0.1 mM EDTA, and 0.1 mM dithiothreitol (pH 7.5)], as shown in Figure S1 of the Supporting Information. The amplified *slyD* DNA, confirmed by agarose gel electrophoresis (Figure S1A, inset) and DNA sequencing during the primer extension experiments (Figure 4A), was precipitated with 7−8 volumes of ethanol; air-dried pellets were then dissolved in purified water to the concentrations indicated below.

In Vitro Transcription. In vitro transcription reactions were conducted in either buffer D [20 mM Tris-acetate, 10 mM magnesium acetate, 50 mM potassium acetate, and 1 mM
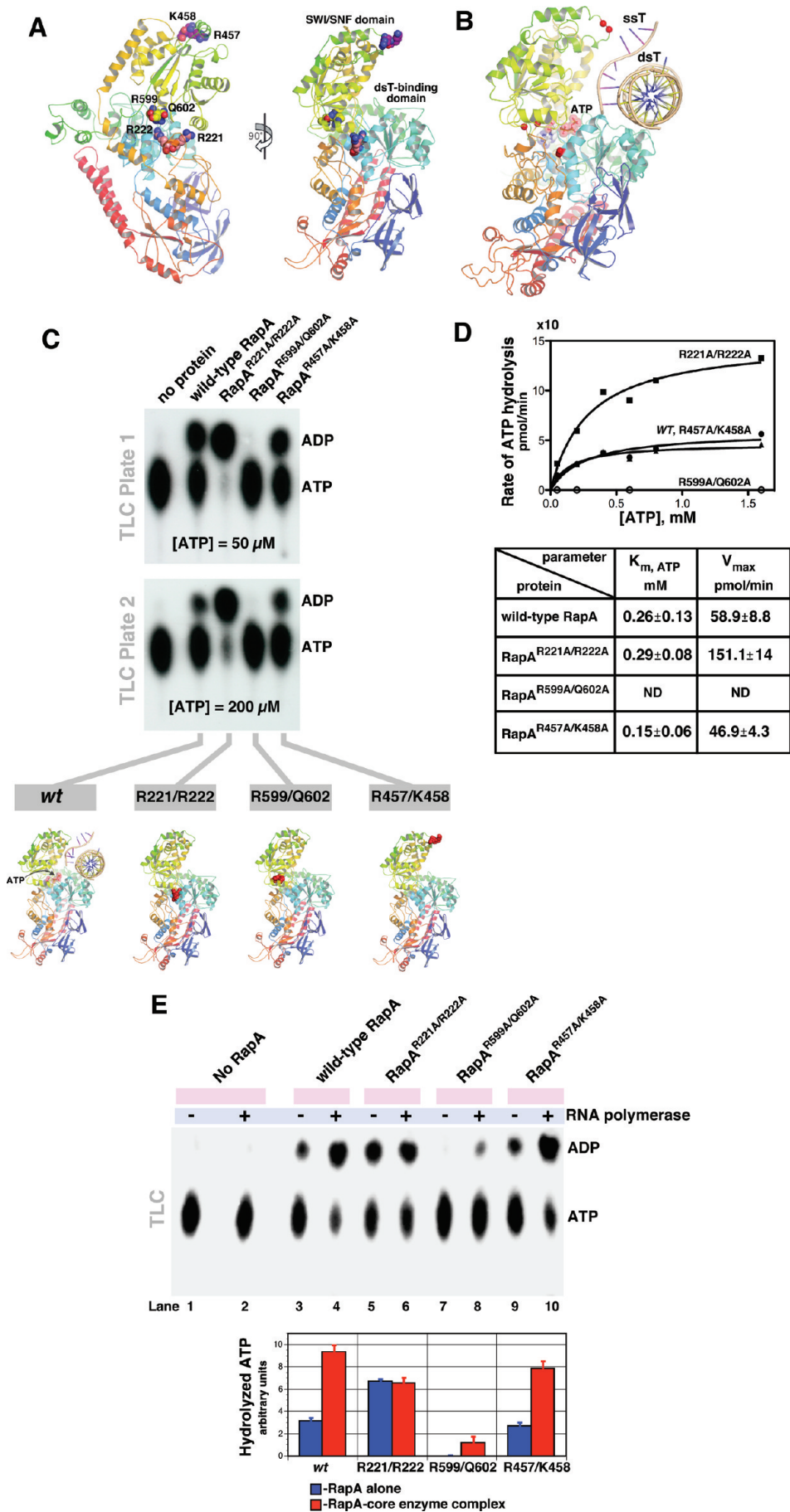
FIGURE 2: Effect of the mutations in RapA's SWI/SNF domain and its interface with the putative double-stranded nucleic acid binding domain on the ATP hydrolytic activity of RapA. (A and B) Positions of the selected mutation sites in the RapA structure. For the sake of clarity, only the backbone of the RapA structure (*18*) is shown; the mutated amino acids are shown as spheres. Panel B also shows the hypothetical positions of a double-stranded nucleic acid template (dsT; a cross-sectional view is shown) and a single-stranded nucleic acid template (ssT). The dsT position (*17, 18*) is determined solely on the basis of modeling using the *Sso*Rad54−DNA complex (*47*) as a template; no available data conclusively rule out RNA as a dsT. ssT binding by RapA's SWI/SNF domain is also supported by the modeling data (*18*). The composite model shown in panel B was constructed as described by Shaw et al. (*18*), essentially by mapping the ATP and nucleic acid binding sites (both single- and double-stranded DNA) from available crystal structures of the ternary PcrA−ATP−DNA and binary *Sso*Rad54−DNA complexes onto the *E. coli* RapA structure (PDB entry 3DMQ), followed by manual adjustment and energy minimization. (C and D) Mutations in the interface of RapA's putative dsT binding and SWI/SNF domains significantly alter its ATP hydrolytic activity. ATPase assays were conducted in buffer D, as described in Materials and Methods. Representative PEI-cellulose plates illustrating the ATP hydrolysis by the wild-type and mutant RapA proteins are shown in panel C. Kinetic parameters (K_m and V_{max}) summarized in panel D were obtained from the initial velocity of ATP hydrolysis vs the ATP concentration plots (shown at the top) using Prism 5 (GraphPad). The parameters were calculated assuming classic Michaelis−Menten kinetics. ND means not detectable. (E) Effect of the core RNA polymerase on the ATP hydrolytic activity of the wild-type and mutant RapA proteins. ATPase assays were conducted in buffer D, as described in Materials and Methods. Reactions without (lanes 1, 3, 5, 7, and 9) or with 2 mol of the purified core RNA polymerase per mole of RapA (lanes 2, 4, 6, 8, and 10) are shown. Quantitated results of the experiment are shown below; data represent the average of two independent sets of experiments.
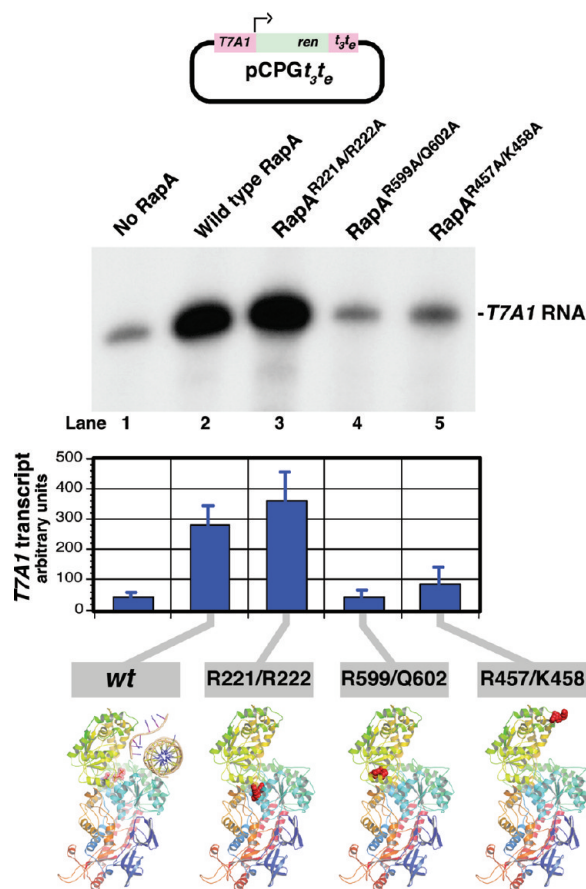

FIGURE 3: Effect of the mutations in RapA's SWI/SNF domain and its interface with the putative double-stranded nucleic acid binding domain on RapA's transcription stimulatory activity. In vitro transcription reactions with the supercoiled DNA template pCPGt_3t_e (*26*) containing the *T7A1* promoter were conducted in buffer C for 60 min in the absence (lane 1) or presence of 0.36 μM recombinant wild-type (lane 2) or mutant RapA proteins (lanes 3−5) as described in Materials and Methods. Supercoiled DNA template at 0.032 μg/μL and purified RNA polymerase holoenzyme at 0.023 μg/μL. Following the addition of stop solution, the reaction mixtures were denatured by boiling and the ^{32}P-labeled RNA transcripts were fractionated on 8% SequaGel (National Diagnostics). Quantitated results of the experiment are shown at the bottom; data represent the average of two independent sets of experiments.

dithiothreitol (pH 7.9)], buffer C [50 mM Tris-HCl, 10 mM MgCl$_2$, 100 mM NaCl, and 1 mM dithiothreitol (pH 7.9)], or buffer B [50 mM Tris-HCl, 10 mM MgCl$_2$, 200 mM NaCl, and 1 mM dithiothreitol (pH 7.9)]; the transcription buffers are specified in the figure legends. In our preliminary studies, we found

that the *slyD* mRNA was more efficiently synthesized in vitro in buffer D than in the previously utilized buffer B (*17*). Since buffer D is widely used as a standard buffer for a large number of bacterial restriction endonucleases and includes potassium and acetate (both key ions in *E. coli*), we switched to buffer D as a more "physiological" buffer for in vitro transcription with linear DNA templates containing the *slyD* operon. Typically, 14 μL in vitro transcription reaction mixtures included 1.4 μL of 10× reaction buffer, 2−4 μL of purified linear DNA template containing the *slyD* operon (20−90 μg/mL in purified water), or 1−2 μL of supercoiled DNA template pCPGt_3t_e (*26*) (0.3−0.4 μg/μL in purified water), 2 μL of purified RNA polymerase holoenzyme (0.07−0.2 mg/mL in 1× TGED buffer, unless indicated otherwise in the figure legends), 0.5−4 μL of purified recombinant RapA (RapA concentrations are specified in the figure legends), and purified water (KD Medical, molecular biology grade) in a volume of 12 μL. In vitro transcription was initiated by the addition of 2 μL of rNTP mix containing ATP, GTP, CTP, UTP, and either [α-^{32}P]ATP or [α-^{32}P]UTP (1.4 mM each) (MP Biomedicals). Reaction mixtures were incubated for 15 min at 37 °C unless indicated otherwise. Transcription reactions were terminated by the addition of an equal volume (14 μL) of stop solution [50% glycerol, 50 mM EDTA, and 0.1% bromophenol blue (pH 7.5)], and 8 μL aliquots of the reaction mixtures were analyzed (without boiling, unless indicated otherwise) on either nondenaturing or semidenaturing polyacrylamide gels. Semidenaturing (0.4 mm thick, 38 cm long) gels were cast using the SequaGel kit (National Diagnostics); the exact polyacrylamide concentrations are specified in the figure legends. Under semidenaturing conditions (Figure 5), increasing the gel thickness and reducing the sample volume led to a significant reduction in the yields of RapA−RNA and RNA polymerase−RapA−RNA complexes; we therefore believe that the complexes in question are not fully denatured by urea in the matrix of a 0.4 mm thick gel during the course of these separations. Gels were typically run at 20−30 W on a Gibco BRL S2 sequencing gel apparatus until bromphenol blue reached the bottom of the gel, unless indicated otherwise. Nondenaturing (1 mm thick, 32 cm long) gels containing 1× TBE (KD Medical) were cast using ProtoGel polyacrylamide mix (National Diagnostics). After electrophoresis on a Gibco BRL SA apparatus, X-ray films (F-BX810, Phenix Research Products) were exposed to "wet" gels covered with plastic wrap. With Kodak BioMax MS screens, typical exposure times were 8−40 h at −80 °C.

Primer Extension Experiments. Primer extension reaction mixtures (20 μL) included 2 μL of 10× M-MuLV reverse transcriptase reaction buffer, 6000−10000 cpm (^{32}P) of end-labeled
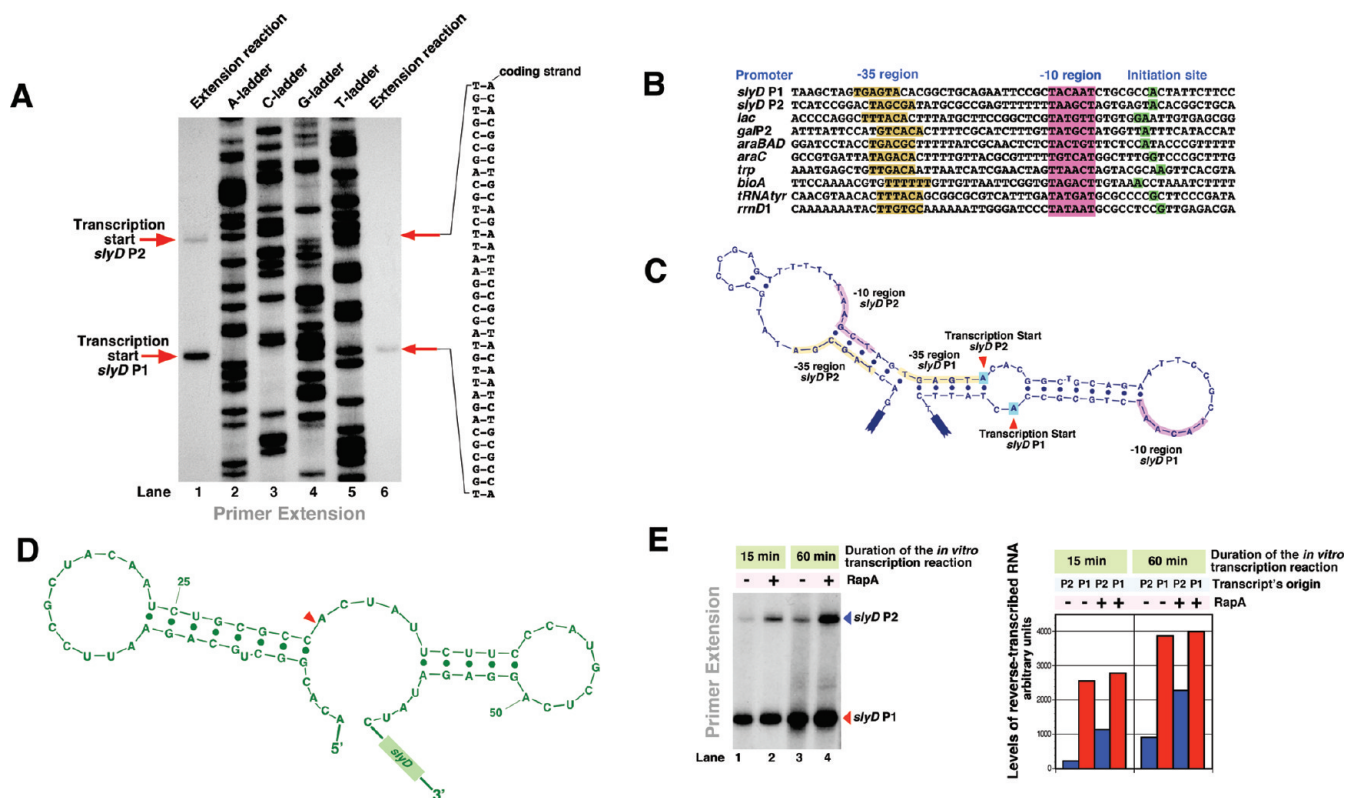
FIGURE 4: Mapping of the transcription initiation site(s) at the *E. coli slyD* operon. (A) Determination of the transcription start site(s) at the *slyD* operon. Primer extension reactions (lanes 1 and 6) resulting from extension of the DNA primer MS702 (see Materials and Methods) by M-MuLV reverse transcriptase from the *slyD* mRNA template(s) synthesized in vitro. Lanes 2−5 show the DNA sequencing ladder, the result of extension of the same primer by *Taq* DNA polymerase. (B) Conserved elements (magenta and yellow boxes) and the transcription start sites (green boxes) of the *slyD* P1 and P2 promoters. *slyD* P1 and *slyD* P2 promoters are aligned against several well-studied *E. coli* promoters. (C) The *slyD* operon's conserved elements and the transcription start sites are shown on the coding DNA strand folded into the hypothetical lowest-energy secondary structure; the template strand is not shown. (D) Nontranslated 5′-terminus of the *slyD* mRNA originating at the P2 promoter. The lowest-energy secondary structure is shown. The red arrowhead points to the 5′-terminus of the *slyD* mRNA originating at the P1 promoter. (E) Effect of RapA on transcription at the *slyD* operon. In vitro transcription reactions were conducted as described in Materials and Methods. Medium-duration (15 min) reactions (lanes 1 and 2) and long-duration (60 min) reactions (lanes 3 and 4) were conducted in the presence or absence of excess (1 μM) wild-type RapA. Primer extension analysis of the RNAs synthesized in vitro was conducted as described in Materials and Methods. Note that RapA has little or no effect on P1-driven transcription but has a positive (4−5-fold) stimulatory effect on transcription initiated at P2. The quantitated levels of reverse-transcribed RNAs are shown at the right.

DNA primer MS702 (5′-CGCGCCAACAGCGACATCAAA-TTTGTCGCC), 2 μL of dNTP mix [containing dATP, dGTP, dCTP, and dTTP (1 mM each)], 2 μL of M-MuLV reverse transcriptase (New England Biolabs, 200000 units/mL), 4 μL of purified RNA from in vitro transcription reactions conducted as described above, and purified water in a final volume of 20 μL. Reaction mixtures were incubated for 30 min at 37 °C, reactions terminated, and mixtures analyzed as described above for in vitro transcription reactions. Labeling and gel purification of the DNA primer MS702 were performed as previously described for end-labeled RNA probes (*17*). Dideoxy-DNA sequencing was conducted as described elsewhere.

Mutagenesis. The QuikChange site-directed mutagenesis kit (Stratagene) was used to construct the described RapA mutations. Primers LZ1 (5′-CAGCATCAGTGGCTGGTAGAA-ATGCTGGCCGCTTTCAACCTGCGCTTTGCGCTATTT-GAT) and LZ2 (antiparallel to LZ1) were used to construct the RapA R221A/R222A double mutation. Primers BY3 (5′-GAG-CAGCGTATTGGTCGTCTGGATGCTATCGGCGCGGC-GCACGATATTCAGATCCATGTG) and BY4 (antiparallel to BY3) were used to construct the RapA R599A/Q602A mutation, and primers BY5 (5′-GCTATTAAAGTCTCCGG-CATTATGGGCGCAGCTGCAAGTGCGGAAGATCGT-GCTCGCGATATGCTC) and BY6 (antiparallel to BY5)

were used to construct the RapA R457A/K458A mutation. Following amplification with mutagenic primers and *Dpn*I digestion of the template DNA [pQE32-RapA (*17*)], aliquots of the reaction mixtures were used to transform XL10-Gold Ultracompetent Cells (Stratagene). Plasmid DNAs from individual clones were purified and analyzed. The constructs were confirmed by DNA sequencing. The expression of full-length RapA in individual clones was also verified by SDS−PAGE−Western blot using RapA-specific antibodies (*14*). The purified plasmids carrying the constructed mutation(s) were then retransformed into M15/pRep4 *E. coli* competent cells (Qiagen), and the His-tagged RapA protein was overproduced and purified as described above.

Western blotting was carried out as follows. Following electrophoresis, proteins were transferred onto either Immobilon-P (Millipore) or Hybond-P (Amersham Pharmacia Biotech) membranes (with similar results) in Mini-PROTEAN 3 Trans-Blot modules (Bio-Rad), typically, at 40−60 V overnight. Membranes were blocked with 5% blotting grade blocker (Bio-Rad, catalog no. 170-6404) in PBST (Calbiochem, catalog no. 524653) for 30−60 min and incubated with primary antibodies (typically, a rabbit serum at a dilution of 1/1000 to 1/5000 in 1× PBST containing 1% blotting grade blocker) for 1−5 h at room temperature on an orbital shaker. Following three 5 min washes with 1× PBST,
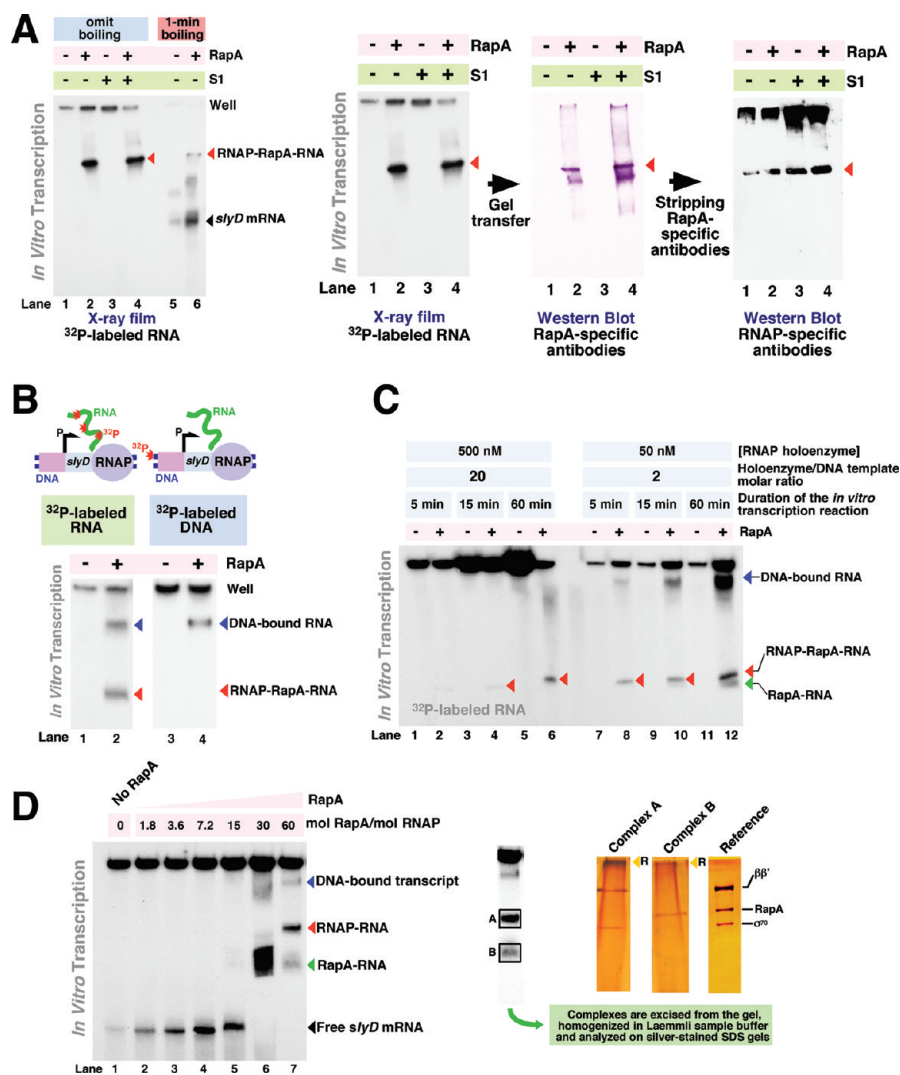
FIGURE 5: RapA contributes to the formation of free (non-DNA-bound or non-aggregated) RNA during in vitro transcription. Fractionation and identification of RapA-specific intermediates under semidenaturing conditions. (A) Formation of RapA-specific complexes in the in vitro transcription system with linear DNA templates encompassing the *E. coli slyD* operon. In vitro transcription reactions without effectors (lanes 1 and 5) or with 1 μM purified recombinant RapA (lanes 2 and 6), 1 μM purified recombinant S1 (lane 3), or 1 μM RapA and 1 μM S1 (lane 4) were conducted as described in Materials and Methods, and the reaction products were separated on 6% SequaGel (National Diagnostics). Reaction conditions: buffer D (see Materials and Methods); purified 965-nucleotide linear DNA template containing the *slyD* operon (PCR MS696/697), 7 nM; RNA polymerase holoenzyme, 20 nM. Reaction mixtures not denatured by boiling are shown in lanes 1−4; reactions in lanes 5 and 6 are identical to those in lanes 1 and 2 except that the samples were subjected to a 1 min boiling step followed by placement on ice after the addition of stop solution. RNA polymerase−RapA−transcript complexes are denoted with red arrowheads. The panels at the right show the identification of the in vitro transcription reaction intermediates through a combination of uniform [^{32}P]RNA labeling and immunoassays. Following electrophoresis, X-ray films were exposed to wet gels to visualize ^{32}P-labeled RNA transcripts. Next, the contents of the gels were electroeluted onto Hybond-P membranes (Amersham Pharmacia Biotech) for immunoassays, first with RapA-specific and next with RNA polymerase-specific antibodies (sequentially, using the same membrane, after the RapA-specific antibodies had been stripped). (B) Identification of DNA-bound complexes formed during in vitro transcription with linear DNA templates encompassing the *slyD* operon through selective ^{32}P labeling of RNA or DNA. In vitro transcription reactions without RapA (lane 1) or with 1 μM purified recombinant RapA (lane 2) were conducted as described in Materials and Methods. Reactions in lanes 3 and 4 were similar to those in lanes 1 and 2 except that ^{32}P end-labeled DNA template and "cold" rNTP mix were used; the experimental design is illustrated by the schematics above. The in vitro transcription reaction products were separated on 4.5% SequaGel (National Diagnostics). (C) Kinetics of the formation of free (non-DNA-bound or non-aggregated) RNA polymerase−transcript complexes in the presence of RapA. In vitro transcription reactions were conducted as described in Materials and Methods in the absence of RapA (lanes 1, 3, 5, 7, 9, and 11) or in the presence of 1 μM wild-type recombinant RapA (lanes 2, 4, 6, 8, 10, and 12), and the reaction products were resolved on 5% SequaGel (National Diagnostics). Reaction conditions: buffer D; purified 965-nucleotide linear DNA template containing the *slyD* operon (PCR MS696/697), 25 nM. The RNA polymerase holoenzyme concentrations are indicated in the figure. The RNA polymerase−RapA−transcript intermediate (red arrowhead), the RapA−RNA adduct (green arrowhead), and the DNA-bound transcript (blue arrowhead) are also indicated. (D) Titration with purified RapA of in vitro transcription reaction mixtures with the *slyD* operon. Reactions were conducted in buffer D, as described in Materials and Methods, and the reaction products were resolved on 4.5% SequaGel (National Diagnostics). Reaction conditions: linear DNA template (PCR 696/697), 40 nM; RNA polymerase holoenzyme, 50 nM. The RNA polymerase−transcript intermediate (red arrowhead), the RapA−RNA adduct (green arrowhead), and the DNA-bound transcript (blue arrowhead) are indicated. The panels at the right confirm the identity of individual complexes; the bands containing ^{32}P-labeled RNA transcript (highlighted by rectangle frames A and B) were dissected from the gel and homogenized in ∼200 μL of Laemmli sample buffer in Eppendorf tube-size disposable homogenizers. Following precipitation of the polyacrylamide slurry by centrifugation, the supernatants were analyzed on silver-stained SDS gels. The reference lane contained the 1:1 RNA polymerase holoenzyme−RapA complex. RapA, σ^{70}, and the large RNA polymerase subunits are indicated; a silver-stained 7% SDS−polyacrylamide gel is shown. Yellow arrowheads (R) indicate RNA, which was also visualized by silver staining.

membranes were incubated with secondary antibodies [a donkey anti-rabbit Ig−horseradish peroxidase conjugate (Amersham Pharmacia Biotech), typically at a dilution of 1/2000 to 1/16000 in 1× PBST containing 1% blotting grade blocker] for 30−60 min. Following three 5 min washes with 1× PBST and two or three brief washes with water, the membranes were incubated for 30 s with 2−4 mL of SuperSignal West Pico Chemiluminescent Substrate (Pierce, catalog no. 34080), briefly drained, and placed in plastic wrap; X-ray films (Phenix Research Products, F-BX810) were then exposed to the luminescent membranes.

ATPase Activity Assays. ATPase activity assays were performed by measuring the amount of [α-^{32}P]ADP released from [α-^{32}P]ATP. Either buffer D or buffer C was used as a reaction buffer, with similar results; reaction buffers are specified in the figure legends. Reaction mixtures (10 μL) contained 1 μL of the 10× reaction buffer, 0.3−0.5 μg of purified RapA, 50−1600 nM cold ATP, and 500−3000 cpm of [α-^{32}P]ATP (MP Biomedicals, catalog no. 32007U). Following incubation at 37 °C (typically for 60 min, unless indicated otherwise in the figure legends), 1.5−3 μL from each reaction mixture was spotted on a PEI-cellulose plate (Analtech, catalog no. 206016), and chromatography was conducted in 1 M LiCl and 1 M formic acid. Following chromatography, the plates were covered with plastic wrap, and X-ray films (Phenix Research Products, F-BX810) were exposed to the TLC plates.

E. coli Strains. The previously constructed MG1655*rapA*$^{-}$ *E. coli* strain (*14*) was used in this work.

RESULTS

Functional Significance of RapA for Bacterial Growth. Although the *rapA* gene is not essential in *E. coli* (*14*), *rapA* deletion results in a unique phenotype manifested as the inability of *E. coli* to grow efficiently on LB agar containing 1 M NaCl (*15*). We recently explained this phenotype in light of our newly rendered model for RapA function in the remodeling of non-canonical DNA−RNA complexes in transcription (*17*), the formation of which is enhanced in high salt (*17*). To study this phenotype further, we (a) analyzed the kinetics of growth of *E. coli* MG1655*rapA*$^{+}$ and MG1655*rapA*$^{-}$ strains on LB agar plates in the presence of NaCl and other salts and (b) compared growth efficiencies of the two strains on agar plates with those in liquid media. Kinetic experiments indicated a pronounced effect of *rapA* on cell growth at ≥0.5 M NaCl. Prolonged incubations of the plates (20−40 h) containing 0.5−0.75 M NaCl resulted in significant differences in colony size between the two strains (Figure 1A). The effects were more pronounced on LB agar plates than on SOC agar or Superbroth agar plates (data not shown). The effect of salts other than NaCl on the growth of the two strains in plated cultures is illustrated in Figure 1B. Interestingly, the growth defect associated with the *rapA* deletion mutation was not evident in the liquid media, under otherwise similar conditions, but was seen only in plated cultures. As an alternative means of increasing the intracellular ionic strength in liquid cultures, we monitored the kinetics of growth of the *rapA*$^{+}$ and *rapA*$^{-}$ strains in the presence of polyethylene glycol. However, these experiments consistently showed little or no difference in growth rates between the two strains, even at relatively high polyethylene glycol concentrations (data not shown).

Alterations of ATP Hydrolytic and Nucleic Acid Remodeling Activities of RapA by Mutations in the Interface

between RapA's SWI/SNF and dsT Binding Domains. We sought to extend previously developed in vitro assays for analysis of the function of individual domains in RapA. Our primary focus was the RapA domain harboring SWI/SNF homology motifs IV−VI (herein termed the SWI/SNF domain), because of its obvious significance in defining the SWI/SNF protein superfamily. Studies with distant homologues of RapA have indicated that coordinated, ATP-driven reorientation of the SWI/SNF domain with respect to the double-stranded nucleic acid binding domain may enable translocation of SNF2 enzymes along nucleic acids (*27, 28*). We therefore sought to genetically alter the interface of the two domains in RapA (Figure 2A,B) to determine the effect of such modifications on RapA's ATP hydrolytic and nucleic acid remodeling activities. With this aim, we constructed and purified two mutant RapA proteins (each carrying a double mutation): RapA$^{R599A/Q602A}$ [this conserved amino acid pair is located within the section of RapA's SWI/SNF domain facing the dsT binding domain (Figure 2A,B)] and RapA$^{R221A/R222A}$ [this moderately conserved arginine tandem is positioned in the section of RapA's dsT binding domain facing the SWI/SNF domain (Figure 2A,B)]. Each double mutation, on the basis of available structural data (*18*), should result in destabilization of the interaction between RapA's dsT binding and SWI/SNF domains. The purification of both mutant proteins is described in the Supporting Information (Figure S2A,B). The second set of mutations targeted a potential single-stranded nucleic acid binding site within RapA's SWI/SNF domain. Recent work indicated that RapA's SWI/SNF domain could be involved in binding single-stranded nucleic acids (*18*). The model of the RapA−nucleic acid complex introduced by Shaw et al. suggests that the loop within RapA's SWI/SNF domain carrying a conserved tandem of positively charged amino acids [R457/K458 (Figure 2A,B)] may be involved in this interaction (*18*). We therefore constructed and purified a RapA mutant carrying alanine substitutions at these two amino acid positions [RapA$^{R457A/K458A}$ (Figure S2C of the Supporting Information)].

Mutations in the interface of RapA's dsT binding and SWI/SNF domains altered ATP hydrolysis by purified RapA, as expected. The RapA R599A/Q602A mutation abolished ATPase activity in purified mutant RapA [Figure 2C,D; the solubility and yields of RapA$^{R599A/Q602A}$ were comparable to those seen with wild-type RapA (Figure S2B,D)]. In contrast, the RapA R221A/R222A mutation resulted in an increase in ATPase activity in the purified protein (Figure 2C,D); the effect was primarily due to an increase in k_{cat} (Figure 2D). Because this is the first case to date in which a RapA mutation resulted in an increase in RapA's specific ATPase activity, we conducted multiple, side-by-side purifications of wild-type RapA and RapA$^{R221A/R222A}$; during the course of these trials, we consistently observed higher specific ATPase activities with purified RapA$^{R221A/R222A}$ (a representative side-by-side comparison of specific ATPase activities in proteins obtained in an independent set of purification procedures is shown in Figure S3 of the Supporting Information). The RapA R457A/K458A double mutation had little or no effect on ATP binding ($K_{m,ATP}$) and hydrolysis (Figure 2D). This result is expected and is consistent with the predicted position of these amino acids in the section of RapA's SWI/SNF domain opposite from the putative ATP binding site (*18*).

Next, we monitored ATP hydrolysis by wild-type and mutant RapA proteins in the presence or absence of ssRNA, a

(ds)RNA−DNA hybrid, and dsDNA. There was no apparent effect of these nucleic acids on the rates of RapA-mediated ATP hydrolysis (Figure S4 of the Supporting Information). This result is in accord with previously reported data indicating little or no modulation of RapA's ATPase activity by nucleic acids (6) [in contrast to the Rad54 homologue from *Sulfolobus solfataricus* (*Sso*Rad54), the ATPase activity of which is stimulated by nucleic acids (29)]. Because it was reported that RNA polymerase exerts a stimulatory effect on the k_{cat} of the RapA ATPase (6), we also monitored the ATP hydrolysis by wild-type and mutant RapA proteins in the presence or absence of RNA polymerase. We found that RapA$^{R221A/R222A}$ (the specific ATPase activity of which was comparable to that of wild-type RapA in the presence of the polymerase) was insensitive to the stimulatory effect of the polymerase (in Figure 2E, compare lanes 3 and 4 to lanes 5 and 6). ATP hydrolysis was detectable in reaction mixtures containing RapA$^{R599A/Q602A}$ in the presence of the polymerase, an apparent partial recovery of the ATP hydrolytic function in the RapA$^{R599A/Q602A}$−core enzyme complex (in Figure 2E, compare lanes 3 and 4 to lanes 7 and 8). The RapA$^{R457A/K458A}$ double mutant mimicked the behavior of wild-type RapA (in Figure 2E, compare lanes 3 and 4 to lanes 9 and 10).

Next, we compared the transcription stimulatory activities of the constructed RapA mutants with that of wild-type RapA. In this set of experiments, we used an extensively characterized supercoiled DNA template (pCPGt_3t_e) containing the *T7A1* promoter (26; also see refs 15−17). In the case of RapA$^{R221A/R222A}$ and RapA$^{R599A/Q602A}$, the effects of the mutations on the transcription stimulatory activity correlated with those on ATP hydrolytic activity (i.e., there was little or no transcription stimulatory effect in the presence of excess RapA$^{R599A/Q602A}$, and there was a transcription stimulatory effect comparable to or exceeding that of wild-type RapA in the case of RapA$^{R221A/R222A}$) (Figure 3). RapA$^{R457A/K458A}$ was largely ineffective in promoting transcriptional cycling under these conditions (in Figure 3, compare lanes 2 and 5), even though its ATP hydrolytic activity was comparable to that of wild-type RapA (Figure 2C,D).

Selection and Characterization of a Model System for in Vitro Transcription of a Complete E. coli Gene. To date, the effects of RapA on the synthesis of relatively long and less structured (i.e., more physiologically relevant) RNAs have not been thoroughly studied. This apparent shortcoming of our previously used model systems prompted us, in this work, to focus on the effects of RapA on the transcription of a complete *E. coli* model gene possessing intact 5′- and 3′-nontranslated sequences. Although a number of model systems for in vitro transcription of *E. coli* genes have been described, they did not fully meet our selection criteria, which included requirements for (a) a robust promoter resulting in a relatively high copy number of the translated protein product, (b) a transcribed gene constituting an independent transcription translation unit (to avoid polar effects in genetic studies), (c) the exhibition of a relatively benign enzymatic activity by the translated protein, and (d) a size of ≤1 kb (to facilitate the analysis of DNA-bound transcription complexes on polyacrylamide gels). After some preliminary work, we selected the *E. coli slyD* gene, which encodes a 21.2 kDa protein bearing the same name [referring to the observation that mutations in the *slyD* gene result in sensitivity to lysis by bacteriophage (30)]. SlyD is an abundant protein chaperone with demonstrated peptidyl-prolyl cis−trans isomerase (rotamase) activity (31−33) and is a frequent contaminant during the metal affinity resin purification of His-tagged proteins (34−36). Indeed, we identified SlyD by mass spectrometry during the purification of recombinant RapA (Figure S1C of the Supporting Information, bottom panel). During the course of our preliminary work, we (a) amplified and purified DNA containing the *slyD* gene and its promoter and confirmed its ability to support a promoter-specific RNA polymerase transcriptional activity (see Figures 5 and 6) and (b) mapped the *slyD* promoter(s) and determined the exact transcription sites for the RNA polymerase holoenzyme by the primer extension method (Figure 4). Primer extension indicated two distinct transcription start sites, both, conventionally, A's (Figure 4A; the nontranslated 5′-termini of the *slyD* mRNAs are shown in Figure 4D). The tandem *slyD* promoters (denoted P1 and P2) share homology with known *E. coli* promoters (Figure 4B). Primer extension experiments indicated little or no non-promoter-specific initiation during in vitro transcription (Figure S5 of the Supporting Information). We also (c) determined the approximate position of the *slyD* gene's transcription terminator (loosely mapped to the tandem hairpins located immediately downstream from the *slyD* gene) (Figure S6 of the Supporting Information); the efficiency of termination in vitro at this intrinsic *slyD* terminator was consistently high (>80%; Figure S6 of the Supporting Information). Taken together, these results are consistent with the existing *E. coli* databases, which indicate that the *slyD* gene is transcribed and translated independently. In summary, the PCR-generated DNA templates encompassing the *slyD* operon met most of our criteria, so we proceeded to the experiments addressing the effects of RapA.

Effect of RapA on Transcription of the slyD Gene in Vitro and Identification of the Reaction Intermediates. (*i*) *Semidenaturing Fractionation of in Vitro Transcription Intermediates.* In our previous work, semidenaturing fractionation of in vitro transcription complexes was instrumental for the detection of RapA−transcript and RNA polymerase−RapA−transcript intermediates (17). We here used a similar approach to test what effect (if any) the addition of purified RapA would have on synthesis of the *slyD* mRNA. In the absence of RapA, RNA polymerase produced little or no detectable non-protein-bound or non-aggregated transcripts in the samples not denatured by boiling (Figure 5A, lanes 1 and 3). In contrast, reaction mixtures containing RapA consistently yielded non-DNA-bound or non-aggregated RNA (Figure 5). Next, we tested whether S1, the RNA binding ribosomal protein capable of stimulating transcriptional cycling [likely, via cooperative interaction with nascent RNA in a cotranscriptional manner (19)], could mimic the observed activity of RapA. These experiments showed that excess S1 failed to promote an RNA release similar to that seen with RapA (resulting in the transcript's appearance as non-DNA-bound or non-aggregated species in gel-fractionated reaction mixtures) (in Figure 5A, compare lanes 2 and 3). On low-percent (<5%) polyacrylamide gels, we were able to discriminate clearly between DNA-bound and non-DNA-bound transcripts through selective ^{32}P RNA or DNA labeling (Figure 5B). The kinetics experiments demonstrated the RNA displacement at early (5 min) time points (Figure 5C, lanes 7 and 8). An increase in the RNA polymerase/DNA template molar ratio, while boosting the overall yield of the transcript, promoted the formation of large complexes incorporating nascent RNA. Nevertheless, the activity of RapA was also apparent at late time points under these conditions (Figure 5C, lanes 3−6). Titration of the in vitro transcription reaction mixtures with purified RapA and

identification of the RapA-specific reaction intermediates are shown in Figure 5D.

(*ii*) *Nondenaturing Fractionation of in Vitro Transcription Intermediates*. To rule out the possibility that the presence of urea accounted for the observed RNA displacement, we conducted PAGE-based fractionations of the in vitro transcription mixtures under nondenaturing conditions (in the absence of urea) (Figure 6A). The ability of RapA to displace ^{32}P-labeled RNA from transcription complexes or aggregates was apparent on nondenaturing gels (Figure 6A); however, a loss of definition in the separation of individual complexes was apparent under nondenaturing conditions.

Next, we compared wild-type RapA with mutant RapA proteins side by side in in vitro transcription reactions with DNA templates containing the *slyD* operon (Figure 6B). In general, the effects of wild-type and mutant RapA proteins on the levels of free (non-DNA-bound or non-aggregated) *slyD* mRNA observed under these conditions were comparable to those seen in in vitro transcription studies with supercoiled DNA template containing the *T7A1* promoter [in which the reaction products were fractionated in the presence of urea (Figure 3)].

We conducted nondenaturing (G-25 Sephadex cartridge-based) purifications of nonproductive transcription complexes containing ^{32}P-labeled RNA transcript (Figure 6C, right panels) and tested their stability in the presence or absence of RapA and ATP. These experiments indicated an ATP-dependent reduction in the levels of DNA-bound or aggregated RNA in the presence of RapA (Figure 6C, graph).

DISCUSSION

RapA, a prokaryotic representative of the SWI/SNF superfamily, was identifed through biochemical studies as a subunit of the *E. coli* RNA polymerase complex (*6*, *14*). In vitro, excess RapA promotes multiround transcription (*15*, *16*). To investigate RapA's nucleic acid substrate specificity and the mechanism of its transcription stimulatory activity, our group analyzed nucleic acid binding and remodeling activities of RNA polymerase−RapA complexes (*17*). In this work, we sought (i) further advances in genetic analyses of RapA (specifically, to extend genetic approaches to understanding the explicit functions of individual RapA domains), (ii) further development of biochemical methods for trapping functionally significant transcriptional intermediates, and (iii) to introduce a model system for in vitro transcription of a complete *E. coli* gene for future biochemical and genetic studies.

Functional Significance of RapA. To obtain additional insights into *rapA* function in vivo, we have further studied the *E. coli* (MG1655) *rapA* deletion strain. Importantly, we demonstrate that the pronounced slow-growth phenotype resulting from the *rapA* deletion mutation is seen only in plated (but not in liquid) cultures. We speculate that this may be due to the *E. coli* cell's improved ability to utilize its ionic pumps in liquid media to lower the intracellular salt concentration (thus reducing the potentially negative impact of salt-induced interactions between nucleic acids). To date, this is the first study demonstrating that the distinct slow-growth phenotype associated with the *rapA* deletion mutation can be observed at physiological osmolarity (Figure 1B). On the basis of this evidence, we argue that the perception of *rapA* as a gene that contributes only marginally to *E. coli* physiology may not be fully correct.

RapA Mutagenesis. RapA mutations described in this work targeted the interface of RapA's putative double-stranded nucleic

template (dsT) binding and SWI/SNF domains and the cluster of positively charged amino acids within RapA's SWI/SNF domain (R457/K458), a tentative single-stranded nucleic acid binding site [and a possible binding site for an RNA strand invading duplex DNA in our model for RapA function (*17*)] (Figure 2B, ssT). Mutations at the interface of RapA's dsT binding and SWI/SNF domains altered RapA's ATPase activity (Figure 2C,D). These results are consistent with the predicted position of RapA's ATP binding site at the interface of the two aforementioned domains (*18*). The constructed mutations also altered the transcription stimulatory activity of RapA and its ability to displace RNA from transcription complexes. In general, the effects of individual mutations on ATP hydrolysis correlated with RapA's transcription stimulatory activity, indicating that the interaction between the SWI/SNF and dsT binding domains may be important for RapA-mediated remodeling of nonproductive transcription complexes. The significant negative effect of the R599A/Q602A double mutation [in the recently reported RapA structure (*18*), these two amino acids are in close proximity to one another] on ATP hydrolysis and the concomitant loss of the protein's transcription stimulatory activity may be due to a general relaxation of the structure of the SWI/SNF domain (as a result of the loss of an internal stabilizing link) and its expansion into the ATP binding cleft. Remarkably, interaction with RNA polymerase enabled partial restoration of RapA[R599A/Q602A]'s ATP hydrolytic function; this result may point to the possibility of reorientation of RapA's SWI/SNF domain with respect to the (putative) double-stranded nucleic acid binding domain, as proposed for the *Sso*Rad54 protein (*27*). The effect of the R221A/R222A mutation, which generated a protein with transcription stimulatory activity exceeding that of wild-type RapA (albeit, insensitive to RNA polymerase regulation), also seems to support the notion that the stimulation of RapA's ATP hydrolytic activity by RNA polymerase may involve reorientation of RapA's SWI/SNF domain with respect to the double-stranded nucleic acid binding domain.

Effects of RapA on in Vitro Transcription of the slyD mRNA. In this work, we developed an in vitro transcription system utilizing a complete model *E. coli* gene (*slyD*). We monitored the in vitro synthesis of *slyD* mRNA and fractionated in vitro transcription reaction intermediates (identified through a combination of selective ^{32}P labeling and immunoassays) by PAGE. Our data unambiguously demonstrate that RapA promotes the formation of non-DNA-bound or non-aggregated RNA species during in vitro transcription (Figures 5 and 6). This result is in accord with the results of our previous study utilizing supercoiled DNA templates and an all-native-enzyme system (*17*). Under most conditions, RapA promoted the formation of (non-DNA-bound) RNA polymerase−transcript complexes. Previously reported RapA−transcript complexes were also detected during the course of this study (e.g., see Figure 5C,D). It seems unlikely that the formation of non-DNA-bound or non-aggregated RNA species in the presence of RapA was due to a general increase in the yield of RNA. (i) Generally, in this set of experiments (Figures 5 and 6), we avoided extended incubations of the in vitro transcription mixtures to minimize potential contributions of RapA to transcriptional cycling. (ii) RapA promoted the formation of the non-DNA-bound or non-aggregated transcript (effectively redistributing RNA in the system) under conditions in which there was clearly no increase in the transcript yield in the presence of RapA (for example, see lanes 3−6 of Figure 5C). (iii) The experiments with the purified
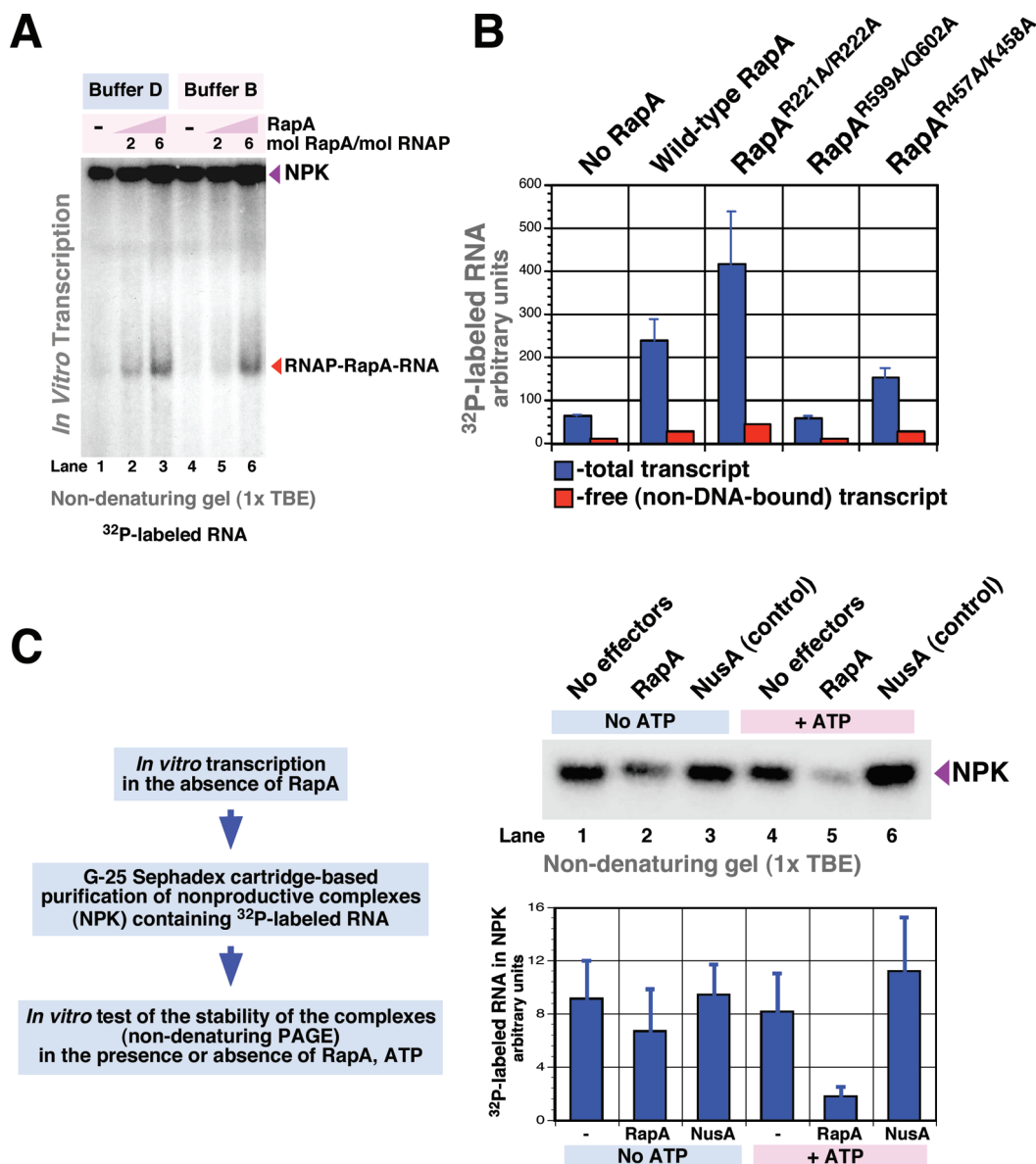
FIGURE 6: RapA contributes to the formation of free (non-DNA-bound or non-aggregated) RNA during in vitro transcription. Fractionation of transcription complexes under nondenaturing conditions. (A) RapA promotes the formation of non-DNA-bound or non-aggregated RNA. In vitro transcription reactions were conducted for 30 min at 37 °C. Reactions 1–3 in buffer D and reactions 4–6 in buffer B (see Materials and Methods). Other components: purified 965-nucleotide linear DNA template containing the *slyD* operon (PCR MS696/697), 25 nM; RNA polymerase holoenzyme, 50 nM. The RapA:RNA polymerase holoenzyme molar ratios are indicated in the figure. Following the addition of stop solution, the reaction products were fractionated on 5% ProtoGel (National Diagnostics) containing $1\times$ TBE (KD Medical), using $0.5\times$ TBE as a running buffer; denaturation of the reaction mixtures by boiling was omitted. (B) Effect of the constructed mutations on RapA's nucleic acid remodeling activity. In vitro transcription reactions similar to those described for panel A were conducted in the presence or absence of 8 mol of wild-type or mutant RapA per mole of RNA polymerase holoenzyme (50 nM). Reaction products were fractionated by nondenaturing PAGE on 8% ProtoGel, as described for panel A. The graph shows the quantitated levels of total ^{32}P-labeled RNA (blue columns) and non-DNA-bound or non-aggregated RNA (red columns). Data represent the average of two independent sets of experiments. (C) Effect of RapA on the stability of purified nonproductive transcription complexes in the presence or absence of ATP. An in vitro transcription reaction similar to that described for lane 1 of panel A was conducted (in the absence of RapA). Following a 30 min incubation, the reaction mixture was diluted to $40\,\mu$L with ultrapure water (KD Medical) and applied to a MicroSpin G-25 column (Amersham Pharmacia Biotech) pre-equilibrated with ultrapure water. Following centrifugation for 2 min at $700g$, approximately $40\,\mu$L of flow-through was recovered (typically containing 3000–8000 cpm of ^{32}P). To test the stability of the purified complexes, $10\,\mu$L reaction mixtures containing $1\times$ buffer C, 500–800 cpm of transcription complexes purified as described above, 1 mM ATP (if present), and $0.2\,\mu$M purified RapA (if present) or NusA (if present, as a control) were incubated for 30 min at 37 °C. Next, 4 μL of stop solution was added to each reaction mixture, and the amount of ^{32}P-labeled RNA retained in the complexes was determined after the samples were fractionated by PAGE on 5% ProtoGel; electrophoresis was conducted as described for panel A. The quantitated data (bottom panel) represent the average of two independent experiments.

nonproductive transcription complexes (Figure 6C) also indicate that RapA contributes to transcript release. Under most experimental conditions, little or no free (non-RNA polymerase-bound or non-aggregated) *slyD* mRNA was generated during in vitro transcription in the absence of RapA, perhaps pointing to

mechanistic limitations in the in vitro synthesis of longer, less structured RNAs.

Function(s) of RapA. The homology of RapA to SWI/SNF proteins and more distant DEAD/H family helicases (*37, 38*) points to roles in nucleic acid remodeling. RapA's status as an

accessory RNA polymerase subunit (*6, 14, 15, 17*) indicates that this nucleic acid remodeling activity is likely linked to transcription. In accord with this, RapA promotes the disruption of noncanonical DNA−RNA complexes (putative DNA−RNA triplexes) in an ATP-dependent manner (*17*). RNA is a likely substrate of RapA, based on multiple, independent lines of evidence summarized in our recent work (*17*). In that study, we proposed that RapA could track DNA along with the RNA polymerase core enzyme to disrupt noncanonical DNA−RNA complexes (*17*). The salt selectivity of RapA's in vivo and in vitro activities supports this model for RapA function.

The results presented herein indicate that RapA contributes to the formation of free (non-DNA-bound or non-aggregated) RNA species during transcription. RNA polymerase without RapA failed to efficiently generate *slyD* mRNA from linear DNA templates containing the *E. coli slyD* operon. Our recent studies suggested that nonproductive interactions by nascent RNA could represent a key obstacle to continuous transcriptional cycling (*19*) (also see ref *17*). In the latter work, we proposed that noncanonical complexes between dsDNA and transcript RNA (such as dsDNA−RNA triplexes) could form during transcription and impede the activity of "trailing" RNA polymerase molecules. The formation of putative dsDNA−ssRNA triplexes is supported by a classic work by Roberts and Crothers (*39*), as well as several recent studies (*17, 40, 41*). RapA-mediated displacement of relatively long transcripts from DNA (as observed in this study under nondenaturing conditions (Figure 6) argues that RapA may possess an independent nucleic acid remodeling activity. The possibility that relatively long transcripts could be wrapped around DNA (in a fashion less orderly than that found in a conventional Hoogsteen triplex) as a result of the polymerase's tracking of a helical, linear DNA molecule has been previously considered (*42*). RapA could disrupt these noncanonical DNA−RNA complexes by either riding with the polymerase while trawling the RNA [Figure 7A, model A1 (the "minesweeper" model)] or acting as a dsDNA−ssRNA topoisomerase (model A2; schematic not shown). Well-documented, nonproductive ternary complexes in which nascent RNA's 3′-end is extruded (*43−45*) also could represent potential substrates for RapA. RapA could contribute to RNA release by either extracting the misaligned RNA or transporting the polymerase along DNA (thus acting as a translocase), both scenarios resulting in realignment of the core enzyme's active site with the 3′-end of the RNA (Figure 7B, model A3) and subsequent RNA release. Finally, the possibility of RapA disrupting complexes formed between transcripts synthesized on different DNA molecules ("in trans") (model B; schematic not shown) also cannot be entirely ruled out.

Both this study and our preceding work point to RNA as a substrate of RapA. It is therefore interesting to question whether the RNA-directed activities of RapA may overlap to some extent with those of Rho, an extensively studied RNA binding protein with established roles in transcription termination (for a review and a complete set of references, see ref *46*), particularly in light of Rho's known ATP-dependent helicase activity with respect to DNA−RNA hybrids and its demonstrated ability to enhance the release of RNA from transcription elongation complexes. Testing RapA and Rho side by side may shed new light on the functions of these two proteins and is likely to be a part of our future studies of *E. coli* transcription.

In summary, in this work we (a) reported in vivo data demonstrating the functional significance of the *rapA* gene under
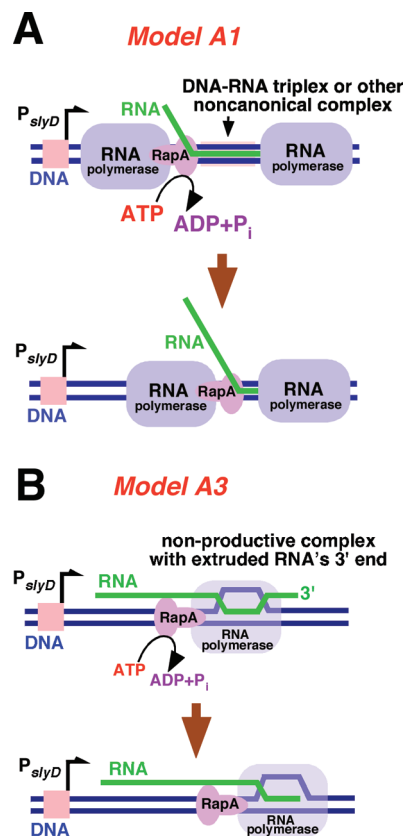

FIGURE 7: Models explaining possible mechanisms of RapA-mediated redistribution of RNA during in vitro transcription. See the text for a detailed discussion of the proposed models. (A) In model A1, RapA lifts the RNA transcript from DNA's major groove and/or unwraps RNA from DNA in a processive manner. (B) In model A3, RapA dissociates nonproductive ternary (DNA−RNA polymerase−RNA) complexes with the extruded 3′-end of RNA by either extracting the misaligned RNA or transporting the polymerase along DNA; both activities could contribute to the redistribution of RNA in the system and reinitiation of transcription.

physiological osmolarity, (b) introduced and characterized a model system for the in vitro synthesis of *E. coli slyD* mRNA and further developed techniques for nondenaturing fractionation of transcription intermediates, and (c) described several new mutations in RapA's SWI/SNF domain and its interface with the (putative) double-stranded nucleic acid template binding domain. The RapA R221A/R222A and R599A/Q602A mutations described in this study (both of which resulted in alterations in RapA's ATPase activity with no apparent effect on protein folding or solubility) represent a valuable asset for future studies. Both mutant proteins, along with the ribosomal protein S1, could serve as controls for ATP-dependent and ATP-independent RapA activities. Finally, (d) in this work, we further refined our models for RapA function in vivo. Our future studies will address the mechanistic aspects of RapA's enzymatic activity in terms of its compatibility with one or more of the models proposed herein. We will also conduct genetic studies designed to identify potential *rapA* interactors in *E. coli*.

SUPPORTING INFORMATION AVAILABLE

Six additional figures. This material is available free of charge via the Internet at http://pubs.acs.org.

REFERENCES

1. Burgess, R. R., Erickson, B., Gentry, D., Gribskov, M. M., Hager, D., Lesley, S., Strickland, M., and Thompson, N. (1987) RNA Polymerase and the Regulation of Transcription , pp 3−15, Elsevier Science Publishing Co., Inc., New York.

2. Gross, C. A., Lonetto, M., and Losick, R. (1992) In Transcriptional Regulation (Yamamoto, K., and McKnight, C., Eds.) pp 129−176, Cold Spring Harbor Laboratory Press, Plainview, NY.

3. Maeda, H., Fujita, N., and Ishihama, A. (2000) Competition among seven *Escherichia coli* σ subunits: Relative binding affinities to the core RNA polymerase. *Nucleic Acids Res. 28*, 3497–3503.

4. Burgess, R. R., Travers, A. A., Dunn, J. J., and Bautz, E. K. (1969) Factor stimulating transcription by RNA polymerase. *Nature 221*, 43–46.

5. Hager, D. A., Jin, D. J., and Burgess, R. R. (1990) Use of Mono Q high-resolution ion-exchange chromatography to obtain highly pure and active *Escherichia coli* RNA polymerase. *Biochemistry 29*, 7890–7894.

6. Sukhodolets, M. V., and Jin, D. (1998) RapA, a novel RNA polymerase-associated protein, is a bacterial homolog of SWI2/SNF2. *J. Biol. Chem. 273*, 7018–7023.

7. Greenblatt, J., and Li, J. (1981) Interaction of the sigma factor and the *nusA* gene protein of *E. coli* with RNA polymerase in the initiation-termination cycle of transcription. *Cell 24*, 421–428.

8. Friedman, D. I., and Gottesman, M. (1983) Lambda II , pp 21−51, Cold Spring Harbor Laboratory Press, Plainview, NY.

9. Muzzin, O., Campbell, E. A., Xia, L., Severinova, E., Darst, S. A., and Severinov, K. (1998) Disruption of *Escherichia coli* hepA, an RNA polymerase-associated protein, causes UV-sensitivity. *J. Biol. Chem. 273*, 15157–15161.

10. Horwitz, R. J., Li, J., and Greenblatt, J. (1987) An elongation control particle containing the N gene transcriptional antitermination protein of bacteriophage lambda. *Cell 51*, 631–641.

11. Squires, C. L., Greenblatt, J., Li, J., Condon, C., and Squires, C. L. (1993) Ribosomal RNA antitermination *in vitro*: Requirement for Nus factors and one or more unidentified cellular components. *Proc. Natl. Acad. Sci. U.S.A. 90*, 970–974.

12. Das, A., Pal, M., Mena, J. G., Whalen, W., Wolska, K., Crossley, R., Rees, W., von Hippel, P. H., Costantino, N., and Court, D.; et al. (1996) Components of multiprotein-RNA complex that controls transcription elongation in *Escherichia coli* phage lambda. *Methods Enzymol. 274*, 374–402

13. Gusarov, I., and Nudler, E. (2001) Control of intrinsic transcription termination by N and NusA: The basic mechanisms. *Cell 107*, 437–449

14. Sukhodolets, M., and Jin, D. (2000) Interaction between RNA polymerase and RapA, a bacterial homolog of SWI2/SNF2. *J. Biol. Chem. 275*, 22090–22097.

15. Sukhodolets, M. V., Cabrera, J. E., Zhi, H., and Jin, D. J. (2001) RapA, a bacterial homolog of SWI2/SNF2, stimulates RNA polymerase recycling in transcription. *Genes Dev. 15*, 3300–3341.

16. Sukhodolets, M. V., Garges, S., and Jin, D. J. (2003) Purification and activity assays of RapA, the RNA polymerase-associated homolog of the SWI/SNF superfamily. *Methods Enzymol. 370*, 283–290.

17. McKinley, B. A., and Sukhodolets, M. V. (2007) *Escherichia coli* RNA polymerase-associated SWI/SNF protein RapA: Evidence for RNA-directed binding and remodeling activity. *Nucleic Acids Res. 35*, 7044–7060.

18. Shaw, G., Gan, J., Zhou, Y., Zhi, H., Subburaman, P., Zhang, R., Joachimiak, A., Jin, D., and Ji, X. (2008) Structure of RapA, a SWI2/SNF2 protein that recycles RNA polymerase during transcription. *Structure 16*, 1417–1427.

19. Sukhodolets, M. V., Garges, S., and Adhya, S. (2006) Ribosomal protein S1 promotes transcriptional cycling. *RNA 12*, 1505–1513.

20. Versteege, I., Sevenet, N., Lange, J., Rousseau-Merck, M. F., Ambros, P., Handgretinger, R., Aurias, A., and Delattre, O. (1998) Truncating mutations of *hSNF5/INI1* in aggressive pediatric cancer. *Nature 394*, 203–206.

21. Sevenet, N., Lellouch-Tubiana, A., Schofield, D., Hoang-Xuan, K., Gessler, M., Birnbaum, D., Jeanpierre, C., Jouvet, A., and Delattre, O. (1999) Spectrum of hSNF5/INI1 somatic mutations in human cancer and genotype-phenotype correlations. *Hum. Mol. Genet. 8*, 2359–2368.

22. Klochendler-Yeivin, A., Fiette, L., Barra, J., Muchardt, C., Babinet, C., and Yaniv, M. (2000) The murine SNF5/INI1 chromatin remodeling factor is essential for embryonic development and tumor suppression. *EMBO Rep. 1*, 500–506.

23. Guidi, C. J., Sands, A. T., Zambrowicz, B. P., Turner, T. K., Demers, D. A., Webster, W., Smith, T. W., Imbalzano, A. N., and Jones, S. N. (2001) Disruption of *INI1* leads to peri-implantation lethality and tumorigenesis in mice. *Mol. Cell. Biol. 21*, 3598–3603.

24. Roberts, C. M. W., Leroux, M. M., Fleming, M. D., and Orkin, S. (2002) Highly penetrant, rapid tumorigenesis through conditional inversion of the tumor suppressor gene *Snf5*. *Cancer Cell 2*, 415–425.

25. Sukhodolets, M. V., and Garges, S. (2003) Interaction of *Escherichia coli* RNA polymerase with the ribosomal protein S1 and the Sm-like ATPase Hfq. *Biochemistry 42*, 8022–8034.

26. Reynolds, R., Bermudez-Cruz, R. M., and Chamberlin, M. J. (1992) Parameters affecting transcription termination by *Escherichia coli* RNA polymerase. I. Analysis of 13 rho-independent terminators. *J. Mol. Biol. 224*, 31–51.

27. Lewis, R., Durr, H., Hopfner, K. P., and Michaelis, J. (2008) Conformational changes of a Swi2/Snf2 ATPase during its mechano-chemical cycle. *Nucleic Acids Res. 36*, 1881–1890.

28. Hopfner, K. P., and Michaelis, J. (2007) Mechanisms of nucleic acid translocases: Lessons from structural biology and single-molecule biophysics. *Curr. Opin. Struct. Biol. 17*, 87–95.

29. Haseltine, C. A., and Kowalczykowski, S. C. (2009) An archaeal Rad54 protein remodels DNA and stimulates DNA strand exchange by RadA. *Nucleic Acids Res. 37*, 2757–2770.

30. Roof, W. D., and Young, R. (1995) jX174 lysis requires *slyD*, a host gene, which is related to the FKBP family of peptidyl-prolyl cis-trans isomerases. *FEMS Microbiol. Rev. 17*, 213–218.

31. Hottenrott, S., Schumann, T., Pluckthun, A., Fischer, G., and Rahfeld, J. U. (1997) *Escherichia coli* SlyD is a metal ion-regulated peptidyl-prolyl *cis/trans*-isomerase. *J. Biol. Chem. 272*, 15697–15701.

32. Scholz, C., Eckert, B., Hagn, F., Schaarschmidt, J., Balbach, J., and Schmid, F. X. (2006) SlyD proteins from different species exhibit high prolyl isomerase and chaperone activities. *Biochemistry 45*, 20–33.

33. Leach, M. R., Zhang, J. W., and Zamble, D. B. (2007) The role of complex formation between the *Escherichia coli* hydrogenase accessory factors HypB and SlyD. *J. Biol. Chem. 282*, 16177–16186.

34. Mitterauer, T., Nanoff, C., Ahorn, H., Freissmuth, M., and Hohenegger, M. (1999) Metal-dependent nucleotide binding to the *Escherichia coli* rotamase SlyD. *Biochem. J. 342*, 33–39.

35. Mukherjee, S., Shukla, A., and Guptasarma, P. (2003) Single-step purification of a protein-folding catalyst, the SlyD peptidyl prolyl isomerase (PPI), from cytoplasmic extracts of *Escherichia coli*. *Biotechnol. Appl. Biochem. 37*, 183–186.

36. Parsy, C. B., Chapman, C. J., Barnes, A. C., Robertson, J. F., and Murray, A. (2007) Two-step method to isolate target recombinant protein from co-purified bacterial contaminant SlyD after immobilized metal affinity chromatography. *J. Chromatogr., B 853*, 314–319.

37. Bork, P., and Koonin, E. V. (1993) An expanding family of helicases within the DEAD/H superfamily. *Nucleic Acids Res. 21*, 751–752.

38. Kolsto, A. B., Bork, P., Kvaloy, K., Lindback, T., Gronstadt, A., Kristensen, T., and Sander, C. (1995) Prokaryotic members of a new family of putative helicases with similarity to transcription activator SNF2. *J. Mol. Biol. 230*, 684–688.

39. Roberts, R. W., and Crothers, D. M. (1992) Stability and properties of double and triple helices: Dramatic effects of RNA or DNA backbone composition. *Science 258*, 1463–1466.

40. Morvan, F., Imbach, J. L., and Rayner, B. (1997) Comparative stability of eight triple helices formed by differently modified DNA or RNA pyrimidine strands and a DNA hairpin. *Antisense Nucleic Acid Drug Dev. 7*, 327–334.

41. Ivanov, S., Alekseev, Y., Bertrand, J. R., Malvy, C., and Gottikh, M. B. (2003) Formation of stable triplexes between purine RNA and pyrimidine oligodeoxyxylonucleotides. *Nucleic Acids Res. 31*, 4256–4263.

42. Drolet, M., Broccoli, S., Rallu, F., Hraiky, C., Fortin, C., Masse, E., and Baaklini, I. (2003) The problem of hypernegative supercoiling and R-loop formation in transcription. *Front. Biosci. 8*, 210–221.

43. Komissarova, N., and Kashlev, M. (1997) Transcriptional arrest: *Escherichia coli* RNA polymerase translocates backward, leaving the 3′ end of the RNA intact and extruded. *Proc. Natl. Acad. Sci. U.S.A. 94*, 1755–1760.

44. Marr, M., and Roberts, J. W. (2000) Function of transcription cleavage factors GreA and GreB at a regulatory pause site. *Mol. Cell 6*, 1275–1285.

45. Nudler, E., Mustaev, A., Lukhtanov, E., and Goldfarb, A. (1997) The RNA-DNA hybrid maintains the register of transcription by preventing backtracking of RNA polymerase. *Cell 89*, 33–41.

46. Banerjee, S., Chalissery, J., Bandey, I., and Sen, R. (2006) Rho-dependent transcription termination: More questions than answers. *J. Microbiol. 44*, 11–22.

47. Durr, H., Korner, C., Muller, M., Hickman, V., and Hopfner, K.-P. (2005) X-ray structure of the *Sulfolobus solfataricus* SWI2/SNF2 ATPase core and its complex with DNA. *Cell 121*, 363–373.